LAWRENCE
LIVERMORE
NATIONAL
LABORATORY

UCRL-TR-207266

# Ground Motion Simulations To Investigate The Feasibility Of Space-Based Seismometry

A. Rodgers

October 15, 2004

This work was performed under the auspices of the U.S. Department of Energy by University of California, Lawrence Livermore National Laboratory under Contract W-7405-Eng-48.

# Ground Motion Simulations To Investigate The Feasibility Of Space-Based Seismometry

Arthur Rodgers
*Earth Sciences Division*
*Lawrence Livermore National Laboratory*

September 15, 2004

**Summary**

This report describes elastic finite-difference simulations of ground motion resulting from explosions and earthquakes for use in a Laboratory Directed Research and Development Feasibility Study (LDRD-FS). The results will be used to as input into further simulations of various spaced-based remote-sensing techniques, such as laser ranging and radar systems. The ground motion calculations involve two types of sources: shallow fully-coupled explosions at relatively shallow depth (1 km) and strike-slip earthquakes at 5 km depth. The event sizes vary from $M_W$ 3.3 to 5.5 to capture a broad range of possible surface motion. The simulations are presented as densely sampled full-field images of ground velocity and displacement as well as peak ground motion versus distance from the event. The resulting peak displacements in the near source region (0-40 km) range from centimeters ($10^{-2}$ m) for the largest events at short ranges to microns ($10^{-6}$ m) for the smallest events at longer ranges. Peak velocities range from centimeters/second ($10^{-2}$ m/s) to micron/second ($10^{-6}$ m/s).

**Introduction**

Seismic source detection, location and identification are among the core capabilities of the Lab. An FY04 mid-year Laboratory Directed Research and Development Feasibility Study (LDRD-FS) project is under way to consider new space-based remote sensing technologies for seismic event observations. As part of this effort we are performing

simulations of Earth surface motions that will be used to assess capabilities of future remote sensing systems.

The simulations are performed with the elastic finite-difference code, *E3D*, developed at LLNL. *E3D* 4th order staggered grid finite difference code (Larsen and Schultz, 1995) and is capable of simulating a wide range of acoustic and elastic wave propagation phenomena. All simulations were performed using the same seismic velocity model. Figure 1 shows the density and seismic P- and S-wave velocities. The grid spacing was set to 0.5 km allowing for accurate simulation up to 0.5 Hz (2 second period).

We chose to simulate both explosion and earthquake ground motions for a range of event sizes. The explosions were placed at 1 km depth to simulate a nuclear weapons test. Using published relations between explosion yield, W, body-wave magnitude, $m_b$, and seismic moment, $M_0$, we determined the seismic moment as a function of explosion yield. We chose to use the yield-mb scaling of Murphy (1996) for tectonic a region:

$$m_b = 4.05 + 0.75 \log[W],$$

where the yield is expressed in kilotons (kT). This will likely lead to an underestimate of the magnitude and is thus somewhat more conservative than choosing the 'stable' region scaling. Patton and Walter (1994) reported a relation between seismic moment, expressed in Newton-meters (N-m) and body-wave magnitude for the Nevada Test Site, also a 'tectonic' region:

$$\log M_0 = 9.55 + 1.12\, m_b$$

Moment magnitude, $M_W$, is related to seismic moment (Kanamori, 1977) by

$$M_W = 2/3\ (\ \log[M_0] + 7\ ) - 10.73.$$

Yields of 1, 10, 50 and 100 kT were chosen for the explosion simulations and seismic moments were computed using the equations given above. For the earthquake simulations we used a strike-slip focal mechanism and 5 km depth. We chose moment magnitudes of the earthquake sources to be equal to those of the explosions. We did not simulate earthquakes larger than $M_W$ 5.5 because such events would likely be spatially extended and violate the assumption of a point source. Table 1 compiles relevant source parameters for the simulations.

**Simulation Results**

We performed eight simulations of explosion and earthquake sources described in Table 1. The experimental set-up and the response of our model to the explosion and earthquake excitation are shown in Figure 2 at a common time step (7.50 seconds). Also shown in Figure 2 are the station locations for theoretical seismograms analyzed below. The peak ground velocity and accelerations on both the vertical and radial (horizontal) components were measured and are plotted versus distance from the source in Figures 3-6. Peak motions ranges from microns ($10^{-6}$ m) to millimeters ($10^{-3}$ m) in displacement and microns/second ($10^{-6}$ m/s) to millimeters/second ($10^{-3}$ m/s) in velocity.

**Acknowledgements**

This effort was supported by a Lawrence Livermore National Laboratory Laboratory Directed Research and Development Feasibility Study (LDRD-FS) project. Bill Foxall and Craig Schultz provided guidance and requirements for the calculations.

**References**

Kanamori, H. (1977). Energy release in great earthquakes, J. Geophys. Res., 82, 2981-2987.

Larsen, S. and C. Schultz (1995). ELAS3D: 2D/3D elastic finite difference wave propagation code, Lawrence Livermore National Laboratory Report, UCRL-MA-121792.

Murphy, J. (1996). Types of seismic events and their source descriptions, in Monitoring a Comprehensive Test Ban Treaty, E. Husebye and A. Dainty (eds.), The Netherlands, 225-245.

Patton, H. and W. Walter (1994). Regional moment:magnitude relations for earthquakes and explosions, Geophys. Res. Lett., 20, 277-280.

**Table 1.** Source parameters for the ground motion simulations.

| # | Source Type | Depth (km) | Yield (kT) | $M_0$ (N-m) | $M_W$ | mb |
|---|---|---|---|---|---|---|
| 1 | explosion | 1.0 | 1 | 1.22e14 | 3.33 | 4.05 |
| 2 | explosion | 1.0 | 10 | 8.43e14 | 3.89 | 4.80 |
| 3 | explosion | 1.0 | 50 | 3.26e15 | 4.27 | 5.32 |
| 4 | explosion | 1.0 | 100 | 5.83e15 | 4.45 | 5.55 |
| 5 | earthquake | 5.0 | - | 1.22e21 | 3.33 | 3.04 |
| 6 | earthquake | 5.0 | - | 8.43e14 | 3.89 | 3.79 |
| 7 | earthquake | 5.0 | - | 3.26e15 | 4.27 | 4.32 |
| 8 | earthquake | 5.0 | - | 5.83e15 | 4.45 | 4.54 |
| 9 | earthquake | 5.0 | - | 3.94e16 | 5.0 | ? |
| 10 | earthquake | 5.0 | - | 2.21e17 | 5.5 | ? |

**Figure Captions**

**Figure 1.** Seismic velocity model used in the ground motion simulations.

**Figure 2.** Comparison of vertical component surface velocities for (a) explosion and (b) earthquake. Also shown are the stations locations (triangles) for theoretical seismograms analyzed in this study.

**Figure 3.** Peak vertical component displacement versus range for the 10 ground motion simulations.

**Figure 4.** Peak horizontal component displacement versus range for the 10 ground motion simulations.

**Figure 5.** Peak vertical component velocity versus range for the 10 ground motion simulations.

**Figure 6.** Peak horizontal component velocity versus range for the 10 ground motion simulations.

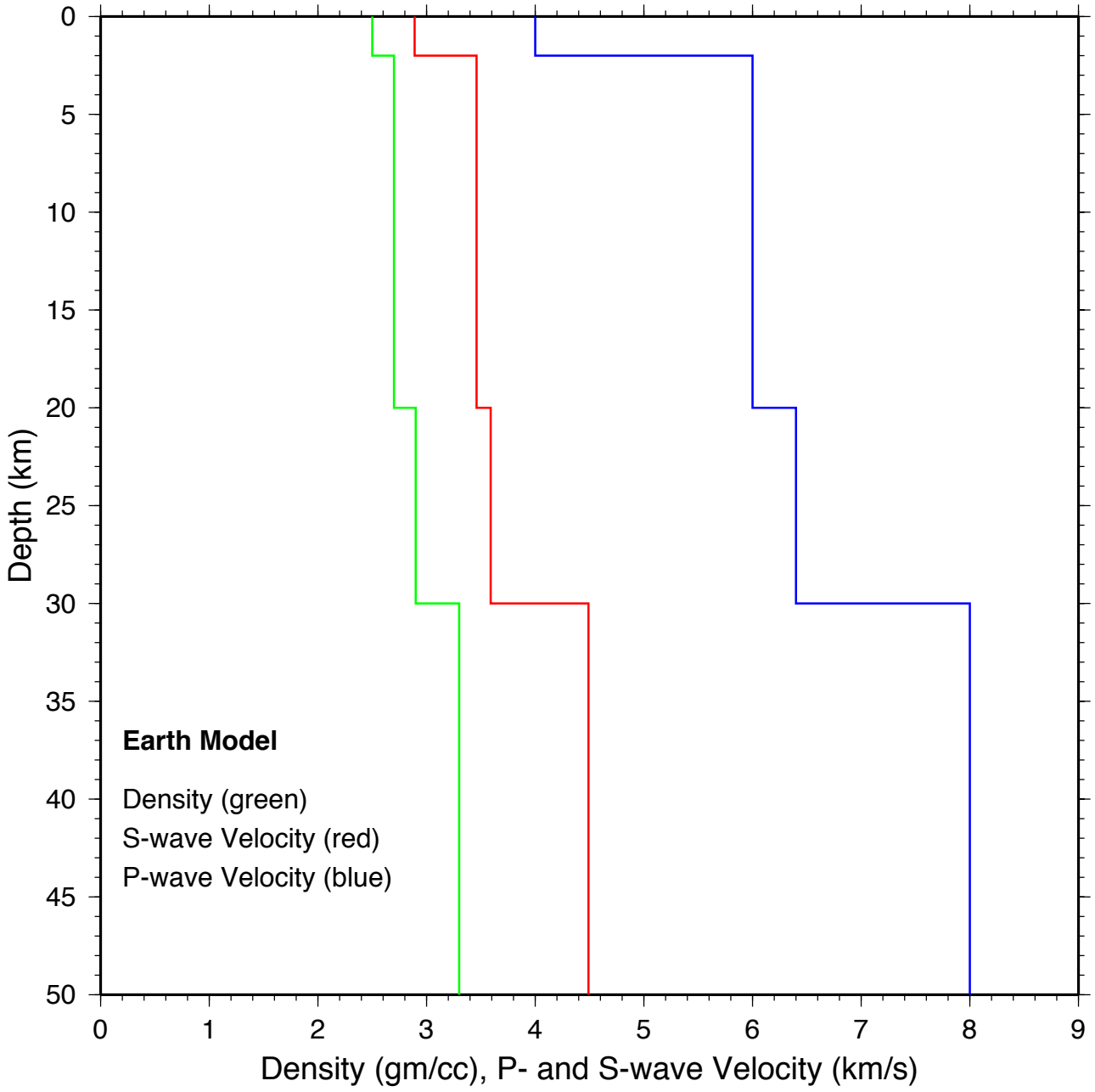


**Figure 1.** Seismic velocity model used in the ground motion simulations.

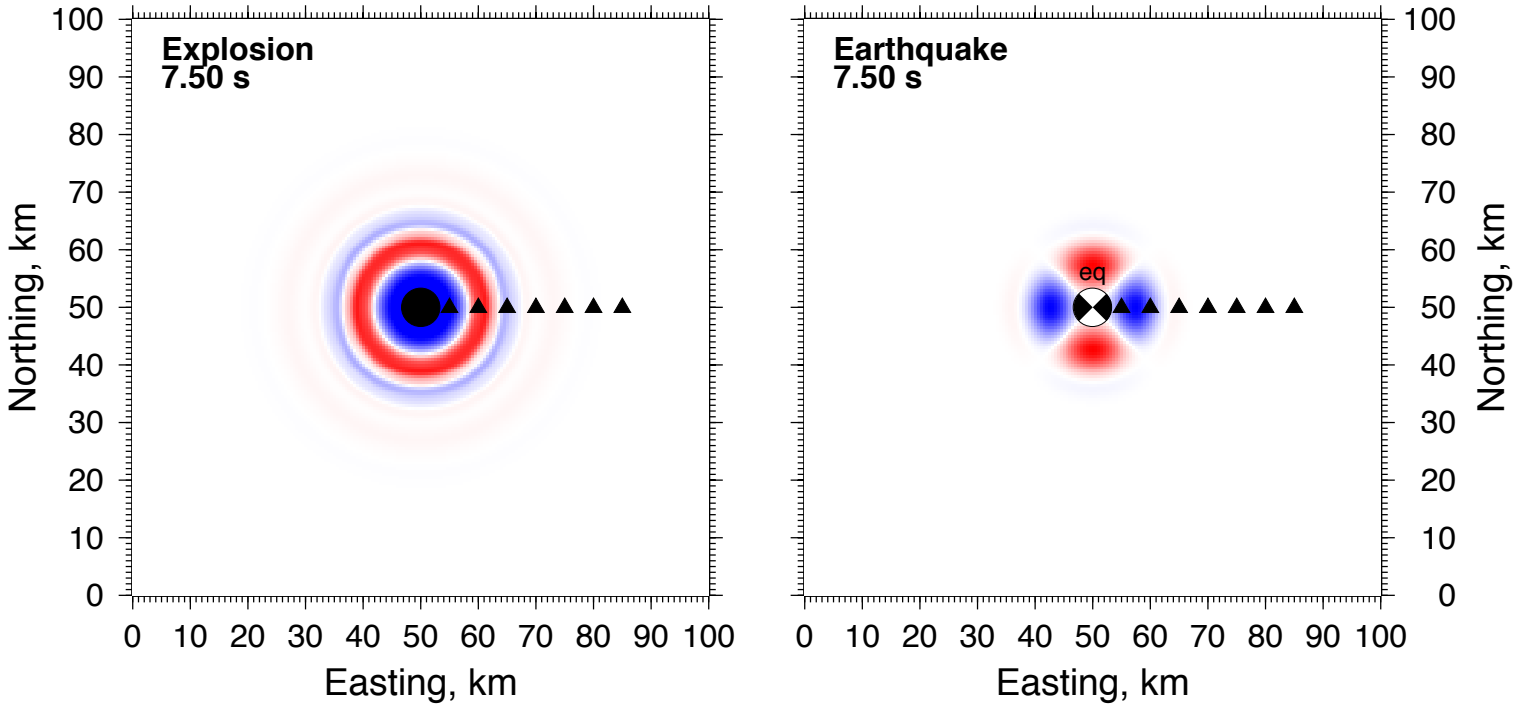


**Figure 2.** Comparison of vertical component surface velocities for (a) explosion and (b) earthquake. Also shown are the stations locations for theoretical seismograms analyzed in this study.

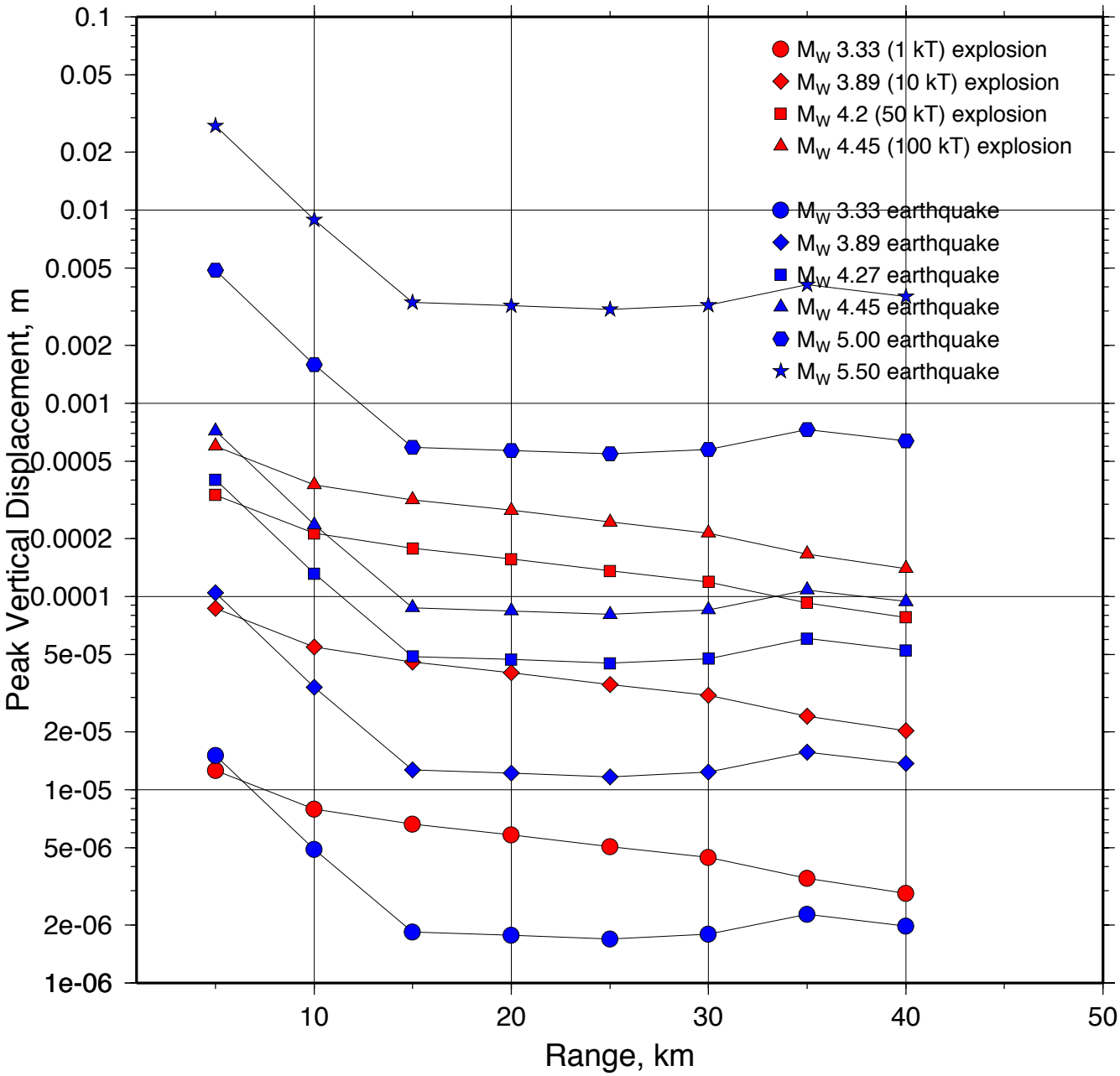


**Figure 3.** Peak vertical component displacement versus range for the 10 ground motion simulations.

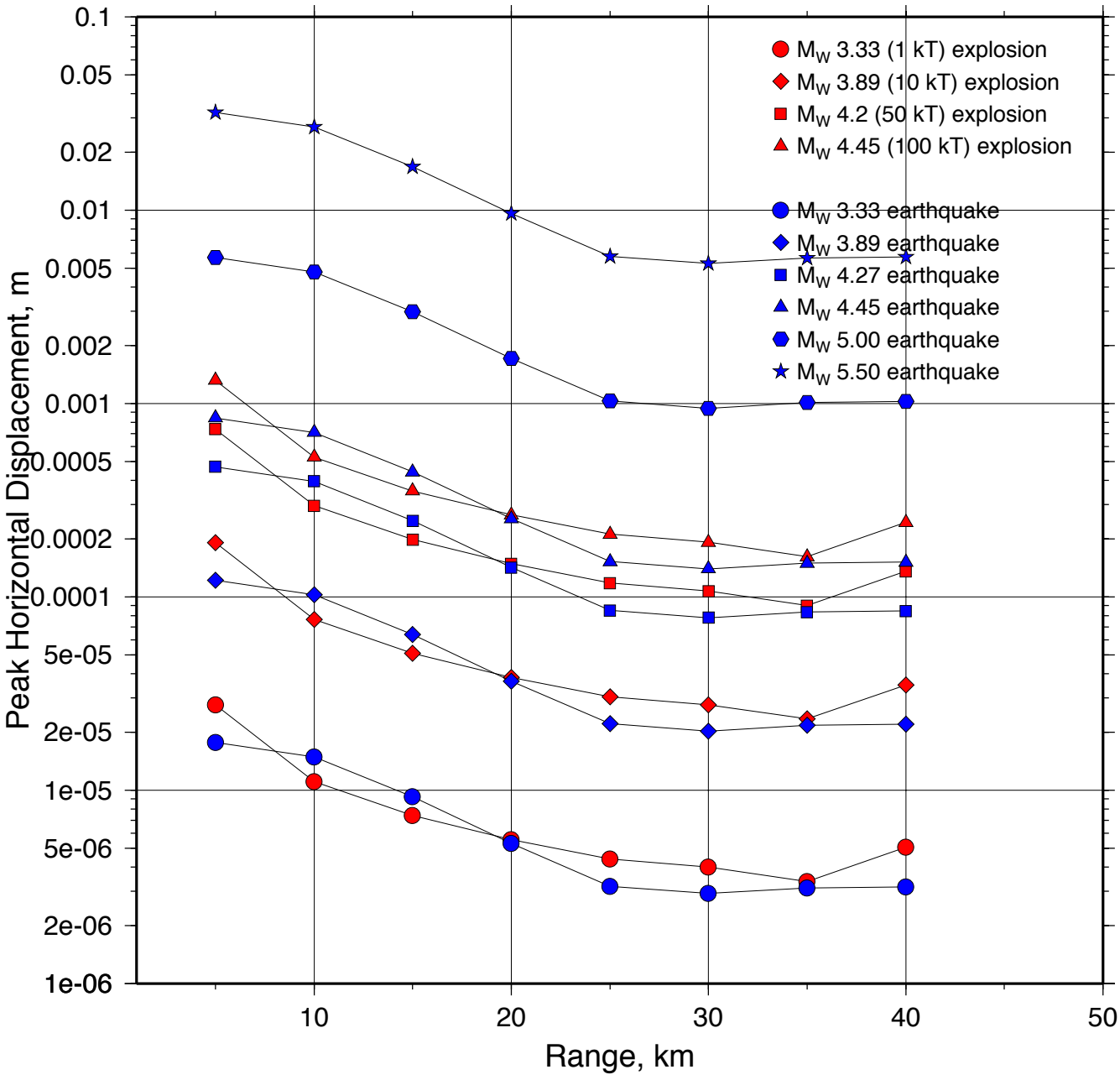


**Figure 4.** Peak horizontal component displacement versus range for the 10 ground motion simulations.

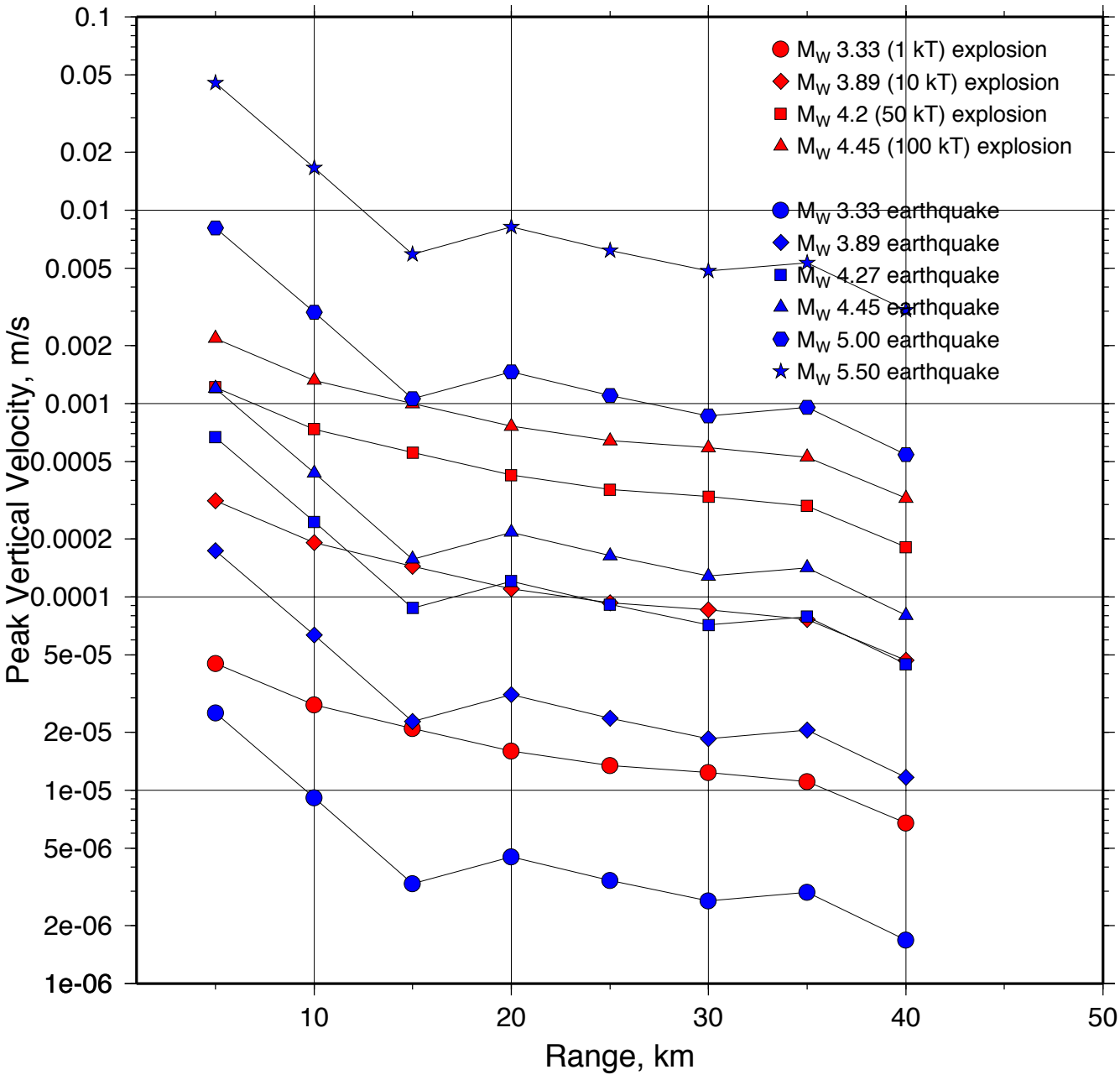


**Figure 5.** Peak vertical component velocity versus range for the 10 ground motion simulations.

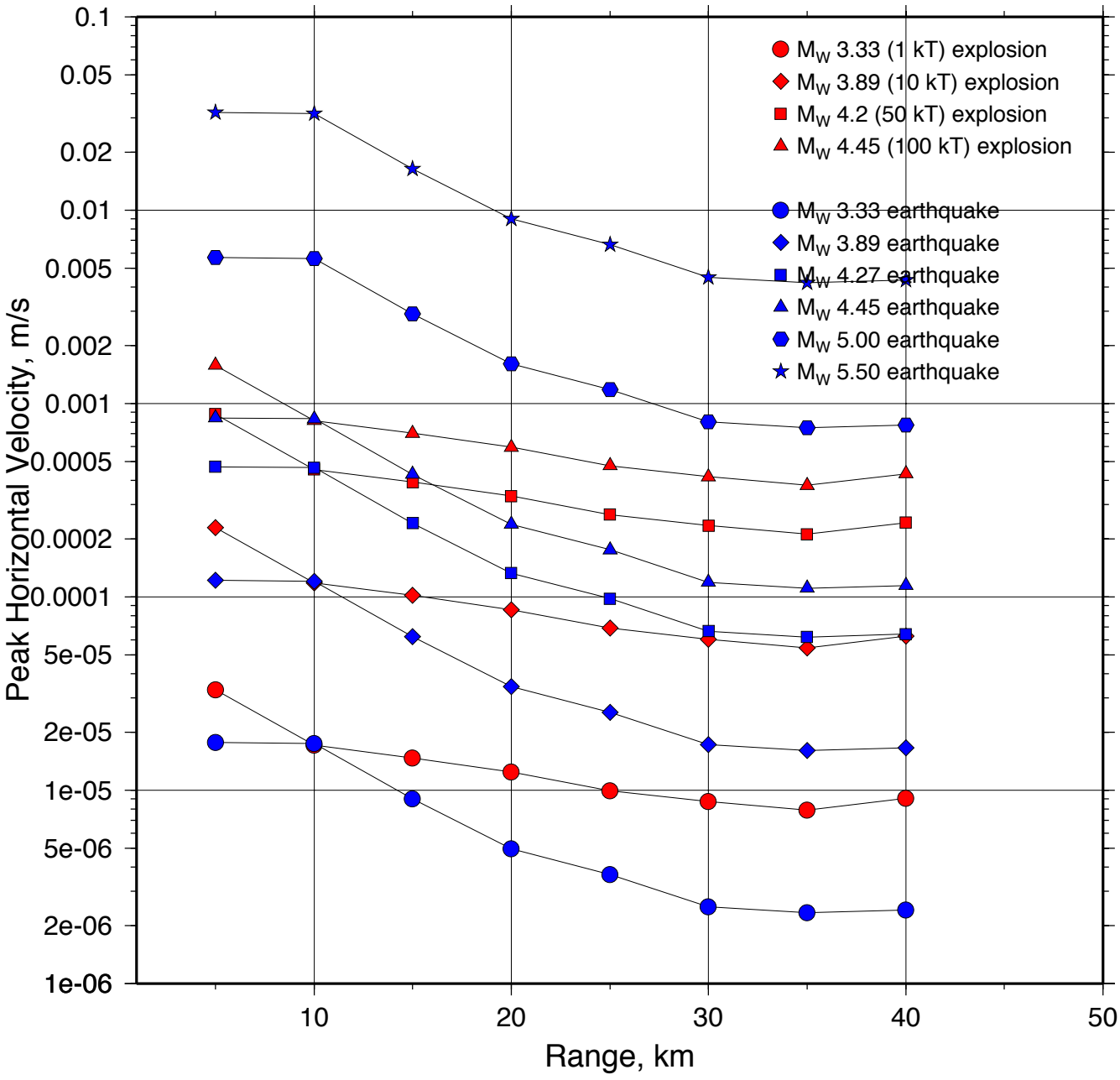


**Figure 6.** Peak horizontal component velocity versus range for the 10 ground motion simulations.